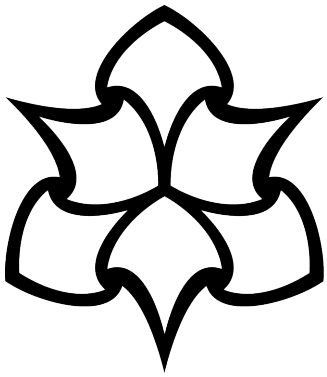

Materials Today Communications 32 (2022) 103879

Contents lists available at ScienceDirect

Materials Today Communications

journal homepage: www.elsevier.com/locate/mtcomm

Scalable solvent-free synthesis of aggregated nanosized single-phase cancrinite zeolite

Ifeoma V. Joseph [a,*], Aidan M. Doyle [a], Abdallah Amedlous [b], Svetlana Mintova [b], Lubomira Tosheva [a,*]

[a] Department of Natural Sciences, Manchester Metropolitan University, Chester St., Manchester M1 5GD, United Kingdom
[b] Normandie University, ENSICAEN, UNICAEN, CNRS, Laboratoire Catalyse et Spectrochimie, Caen 14000, France

ARTICLE INFO

Keywords:
Zeolites
Solvent-free synthesis
Cancrinite
Morphology

ABSTRACT

Pure cancrinite zeolite was prepared using a solvent-free method from a geophagic clay. The morphology of the zeolite could be controlled through the composition of the raw mixture. Aluminum sulfate octadecahydrate was used for the first time as a source of trace water in the solvent-free synthesis of a zeolite. Aggregated nanosized single-phase cancrinite zeolite were prepared using a mixture of the clay, aluminum sulfate octadecahydrate and sodium hydroxide. The mixture was manually mixed and heated at 150 °C for 6 h. Scaling up the synthesis to 2, 4 and 8 times resulted in products with remarkably consistent textural characteristics. The cancrinite prepared showed potential for use as a low-cost adsorbent for CO_2 capture at very low CO_2 concentrations.

1. Introduction

Synthetic zeolites have transformed the modern chemical industry through their use as shape-selective catalysts for crude oil conversion, ion-exchangers and in adsorption and separation processes. Conventionally, zeolites are prepared via hydrothermal treatment of aluminosilicate gels or solutions in an alkaline environment at 80–200 °C for several hours to several days [1]. The drawbacks of conventional zeolite synthesis include low space−time yield, significant waste generation, energy consumption and use of hazardous high-pressure reactors. Recently, efforts have been directed towards the development of green methods for zeolite synthesis [2]. Notably, the solvent-free method has been demonstrated to offer a very attractive alternative to conventional synthesis as discussed in detail in the Account by Wu et al. [3]. In this method, raw zeolite precursor solids are mixed, ground and heated to form a single zeolite phase. The presence of traces of water, either introduced through the use of hydrated silica solids [4] or formed in-situ from anhydrous raw solids in the presence of NH_4F [5] plays an essential role for the zeolite crystallization.

Despite the numerous advantages of the solvent-free method and its successful application to many zeolitic structures, there are limited reports on possibilities to control zeolite morphology and upscaling when this method is used. Luo et al. have demonstrated that aggregates of nanosized ZSM-5 crystals can be prepared from anhydrous solids in the presence of sodium carbonate decahydrate [6]. The morphology could also be controlled by adding additives to the solid mixture such as graphene oxide [7] and urea [8]. Gao et al. have reported the preparation of MOR zeolite by a solvent-free method and have shown that the products of the 10 fold and 100 fold synthesis were also crystalline MOR zeolites, although the product characteristics were not compared in detail [9]. Interestingly, the authors found that the reactor volume had a significant effect on the crystallinity and phase purity of the products.

Herein, we demonstrate that the zeolite morphology in the solvent-free synthesis method can be controlled by changing the trace water-bearing solid. We used aluminum sulfate octadecahydrate as a source of trace water, as opposed to sodium carbonate decahydrate, to drastically change the CAN morphology from the typical rod-like hexagonal crystals to nanosized aggregated crystals; the former trace water source has not been used before in the solvent-free synthesis of zeolites. We have selected cancrinite (CAN) zeolite to prove our concept because this zeolite can be prepared using cheap precursor solids such as natural clays, fly ash, diatomaceous earth, and loess [10–17]. CAN zeolite contains 1-dimensional 12-membered ring 5.9 × 5.9 Å channels, surrounded by ε-cages built up from 6-membered rings and 4-membered rings [18–20]. The large channels and the ε-cages are occupied by anions and cations such as Na^+, OH^-, CO_3^{2-}, SO_4^{2-}, and water. Cancrinite has shown potential for applications in heavy metals removal from water, soil remediation and catalysis [10,14,15,17,21].

* Corresponding authors.
E-mail addresses: i.joseph@mmu.ac.uk (I.V. Joseph), l.tosheva@mmu.ac.uk (L. Tosheva).

https://doi.org/10.1016/j.mtcomm.2022.103879
Received 25 January 2022; Received in revised form 30 May 2022; Accepted 17 June 2022
Available online 20 June 2022

Cancrinite zeolite has been prepared by solvent methods before. Liu et al. reported the preparation of micron-sized hydroxycancrinite (1 μm) spheres from blast furnace slag [22]. The synthesis involved multi-step preliminary treatment to obtain an aluminosilicate gel, which was dried prior its use in the solvent-free synthesis. Cheng et al. prepared CAN from $SiO_2{\cdot}H_2O$, $NaAlO_2$ and NaOH, however, the crystallization and the material characteristics were not studied in detail [21]. Cancrinite aggregated nanosized hexagonal crystals (200 nm) were prepared from rice husk ash (RHA), $NaAlO_2$ and $Na_2CO_3{\cdot}10H_2O$ [23]. This process has some limitations such as a high temperature pre-treatment of the RHA and a relatively long treatment time (48 h at 100 °C). Our method reported here employs a solid mixture made up of a natural clay, sodium aluminate or aluminum sulfate octadecahydrate for adjustment of the Si/Al ratio, and sodium carbonate decahydrate or sodium hydroxide as alkaline sources. Variations of the composition have shed light upon the cancrinite crystallization process. Further, we studied in detail the characteristics of CAN products prepared using different scaling factors of the solid mixture to evaluate scalability of the developed method.

2. Experimental section

2.1. Materials and methods

The clay used in this work was obtained from Anambra, Nigeria. 99.99% purity analytical grades of sodium hydroxide, sodium carbonate, sodium carbonate decahydrate, and aluminum sulfate octadecahydrate powders were purchased from Sigma Aldrich.

The clay was crushed and sieved to particle sizes < 150 μm and used in its as-received form. Predetermined amounts of clay, sodium hydroxide, and aluminum sulfate octadecahydrate (mass ratios of 1.00:1.20:1.45, respectively) were manually mixed in a mortar, placed in Teflon-lined autoclaves, and heated at 180 °C for 0.5–72 h to optimize treatment time, or between 80 and 180 °C for 6 h for optimization of the treatment temperature. Upscaling experiments (1x, 2x, 4x and 8x) were performed as described with heating at 150 °C for 6 h. For the upscaling experiments, the 1x synthesis used 2 g of clay, whereas 16 g of clay were used for the 8x synthesis. Experiments were also carried out using the clay mixed with sodium hydroxide (1.00:1.20 mass ratio), sodium carbonate (1:1.2 mass ratio), sodium carbonate decahydrate (1.00:1.20 mass ratio), or a combination of sodium carbonate decahydrate and sodium aluminate (1.00:1.20:0.13 mass ratio, respectively). The experiments followed the above procedure with heating at 180 °C for 24 h. After the heating, the autoclaves were quenched under running cold tap water, the samples were washed by 5-times centrifugation at 3800 rpm for 5 min and redispersion in distilled water, dried in air, and calcined at 600 °C for 1 h.

2.2. Characterization

Compositional characterization was performed with a Rigaku NEX-CG X-ray fluorescence (XRF). X-ray diffraction (XRD) patterns were collected with an X′Pert PANalytical instrument using Cu Kα at a continuous scan step size of 0.01313° from 10° to 60° 2θ. The XRD patterns were processed with the Malvern HighScore Plus software (version 4.9) using the Crystallography Open Database (COD). Scanning electron microscopy (SEM) images were obtained with a Carl Zeiss Supra 40 V scanning electron microscope. Nitrogen adsorption isotherm measurements at − 196 °C were performed with a Micrometrics ASAP 2020 instrument. Samples were degassed at 350 °C for 3 h prior to analysis. Surface areas were calculated using the Brunauer-Emmett-Teller (BET) method, whereas Barrett–Joyner–Halenda (BJH) pore size distributions were determined from the desorption branch of the isotherms. Micropore volumes and external surface areas were determined by the t-plot method. Transmission electron microscopy (TEM) images were obtained with a Thermo Fisher Talos F200X microscope equipped with an X-FEG electron source. The experiment was performed using an acceleration voltage of 200 kV with a 100 μm C2 aperture and a beam current of approximately 0.5 nA.

In situ Fourier-transform infrared (FTIR) spectra were recorded with a Nicolet 6700 IR spectrometer equipped with a mercury cadmium telluride (MCT) detector. The spectra were recorded in the range of 400–4000 cm^{-1} at a resolution of 4 cm^{-1} after an accumulation of 256 scans. The cancrinite sample (4x sample) was pressed into a self-supported pellet (diameter = 2 cm, weight = 20 mg) and activated in the IR cell. The sample was activated at 250 °C (heating ramp: 5 °C min^{-1}, holding time: 6 h), under vacuum prior to gas adsorption tests. Afterwards the sample was cooled down to 25 °C for the collection of IR spectra upon CO_2 adsorption at CO_2 pressures in the range 1.2–100 torr. All spectra were normalized to the sample mass. CO_2 and N_2 adsorption isotherms were also recorded at 25 °C on a Micromeritics 3Flex Surface Characterization unit (Norcross, GA). The 4x sample was degassed at 400 °C under vacuum for at least 8 h prior to measurement.

3. Results and discussion

A geophagic clay from Anambra, South Eastern Nigeria was used in this study. The characteristics of the untreated clay sample were studied in detail in our previous work [24]. It contained vermiculite, quartz, and kaolinite, 43.9 wt% SiO_2 and 15.1 wt% Al_2O_3 and its BET surface area was 95 $m^2\,g^{-1}$. We used this clay previously to prepare FAU zeolite [24]. The FAU synthesis required an alkali fusion at 600 °C to convert the insoluble crystalline phases into amorphous aluminosilicates prior to crystallization [25]. Such a step was not required in the present study suggesting that the absence of water significantly influences the phase transformations within the closed solid mixture. Selected XRD patterns of samples prepared using different solid mixtures are shown in Fig. 1. Sodium hydroxide and sodium carbonate were used as alkaline sources in the mixtures. The use of sodium hydroxide resulted in the formation of sodalite only (XRD pattern (i)), which has been reported to precede cancrinite during hydrothermal crystallization [26]. Replacing NaOH by anhydrous sodium carbonate did not result in a zeolite phase, but resulted in the formation of an aluminosilicate dense phase and quartz (XRD pattern (ii)). Replacing anhydrous sodium carbonate with its decahydrate salt resulted in the formation of cancrinite mixed with amorphous material and quartz (XRD pattern (iii)). Pure cancrinite could be obtained from this system after the addition of sodium aluminate to adjust the Si/Al ratio. Cancrinite as a single phase was obtained in the presence of sodium carbonate decahydrate and sodium aluminate (XRD pattern (iv)) or sodium hydroxide and aluminum sulfate octadecahydrate (XRD pattern (v)). The conclusions drawn from these experiments are that: (i) the initial Si/Al ratio has an important role for the zeolite crystallization process and has an effect on the formation of dense crystalline phases; (ii) the presence of water traces is essential for the formation of cancrinite; (iii) both sodium hydroxide and sodium carbonate decahydrate can be used as alkaline sources in the solid mixtures but the molar composition of the solid mixture needs corresponding adjustments. The presence of a trace of water in the solvent-free synthesis of zeolites has been found to be essential in previous studies [4]. It has been proposed that a trace of water takes part in the hydration / condensation of silica species during the zeolite crystallization process and can be considered as a catalyst for the zeolite crystallization [3].

The morphology of the cancrinite zeolites obtained was also strongly affected by the initial solid mixture (Fig. 1b and c). Hexagonal nanorods with a length of ca. 1 μm were obtained for the synthesis in the presence of clay, sodium carbonate decahydrate and sodium aluminate (Fig. 1b). The synthesis of such uniform cancrinite nanorods has rarely been reported in the literature [27]. The morphology of the sample prepared in the presence of sodium hydroxide and aluminum sulfate octadecahydrate was aggregated cancrinite nanocrystals with sizes between 30 and 100 nm (Fig. 1c). The difference between the two samples is in the way

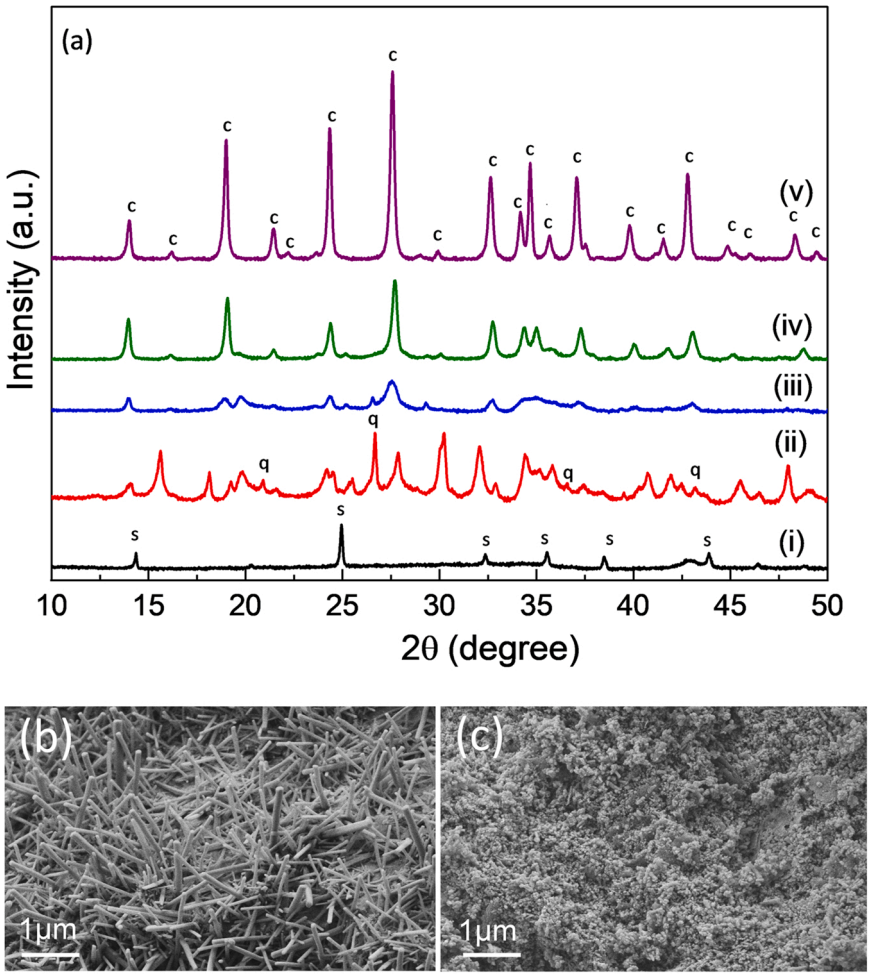

Fig. 1. (a) XRD patterns of samples prepared from solid mixtures treated at 180 °C for 24 h consisting of: (i) clay + NaOH, (ii) clay + Na_2CO_3, (iii) clay + $Na_2CO_3{\cdot}10H_2O$ (iv) clay + $Na_2CO_3{\cdot}10H_2O$ + $NaAlO_2$ and (v) clay + NaOH + $Al_2(SO_4)_3{\cdot}18H_2O$, and SEM images of samples corresponding to XRD patterns (iv) (b) and (v) (c). s: sodalite; q: quartz; c: cancrinite.

the trace water is introduced into the solid mixture, through the alkaline or the aluminum source. The calculated amount of trace water in the two solid mixtures is very similar. In the case of using aluminum sulfate octadecahydrate, the sodium hydroxide provides a more basic environment, which, combined with "aluminum trace water" enhances Si-Al interactions and results in a fast nucleation rate and a large number of viable nuclei, which can then grow but only until nutrients have been consumed [20]. In the case of "sodium carbonate water", fewer nuclei are formed, which grow into larger rod-like crystals.

Owing to the interest in developing nanozeolites, particularly in the absence of organic templates [28,29], and the less explored control of crystal size in the solvent-free method, we have further studied the cancrinite synthesis that results in nanocrystals. We have systematically changed the treatment time at 180 °C between 30 min and 72 h to find the optimal treatment time (Fig. S1, Supporting Information). Cancrinite peaks of low intensity were present in the XRD pattern of the sample prepared for 30 min together with traces of quartz. The peak intensities increased for the samples prepared for up to 6 h and no presence of quartz was detected in the 3 h sample. The XRD patterns of the samples prepared for 6 – 72 h were very similar and indicated the presence of cancrinite as a single phase. XRF analysis showed consistent chemical composition of all samples with a Si/Al ratio changing from 1.73 for the 0 h sample to 1.03 ± 0.02 for the samples prepared between 30 min and 72 h. The results confirm our hypothesis for fast nucleation and suggest solid-state conversion to cancrinite. Synthesis was also performed for 6 h of treatment at different temperatures to establish the lowest temperature that could be used to prepare pure cancrinite. Fig. S2 (Supporting Information) shows that the samples prepared at 80 – 120 °C for 6 h contained quartz impurity and a certain degree of amorphous material, whereas the samples prepared at 150 °C and 180 °C contained cancrinite as a single phase. Again, XRF showed minor variations in the chemical composition of the samples prepared at different temperatures.

From the above experiments, the optimal conditions of treatment at 150 °C for 6 h were used to prepare samples with 1x, 2x, 4x and 8x scaling factors, starting with 2, 4, 8 and 16 g of clay. The XRD patterns and typical SEM and TEM images of these samples are shown in Fig. 2. XRD analysis indicated that cancrinite was present as a single phase in all samples (Fig. 2a). All samples consisted of aggregated nanoparticles with a size between 30 and 100 nm, although isolated nanorods were also observed in both the SEM and TEM images (Fig. 2b and c and Fig. S3, Supporting Information). An average crystallite size of 36 ± 3 nm was calculated in HighScore Plus by line profile analysis of the cancrinite (211) peak using a Pseudo-Voight peak function (Table 1). The Si/Al ratios of all samples was 1.02 and the cancrinite channels were filled with similar amounts of sulfate ions. The samples had negligible micropore volumes, $< 0.004\ cm^3\ g^{-1}$, which is typical for cancrinite zeolites because of their anion fillings [20]. However, the materials prepared in this work showed high surface areas for cancrinite, 61 ± 3 $m^2\ g^{-1}$, because of their high external areas, 54 ± 2 $m^2\ g^{-1}$, associated with textural porosity due to the nanosized crystals [29]. Nitrogen adsorption desorption isotherms and BJH pore-size distributions of

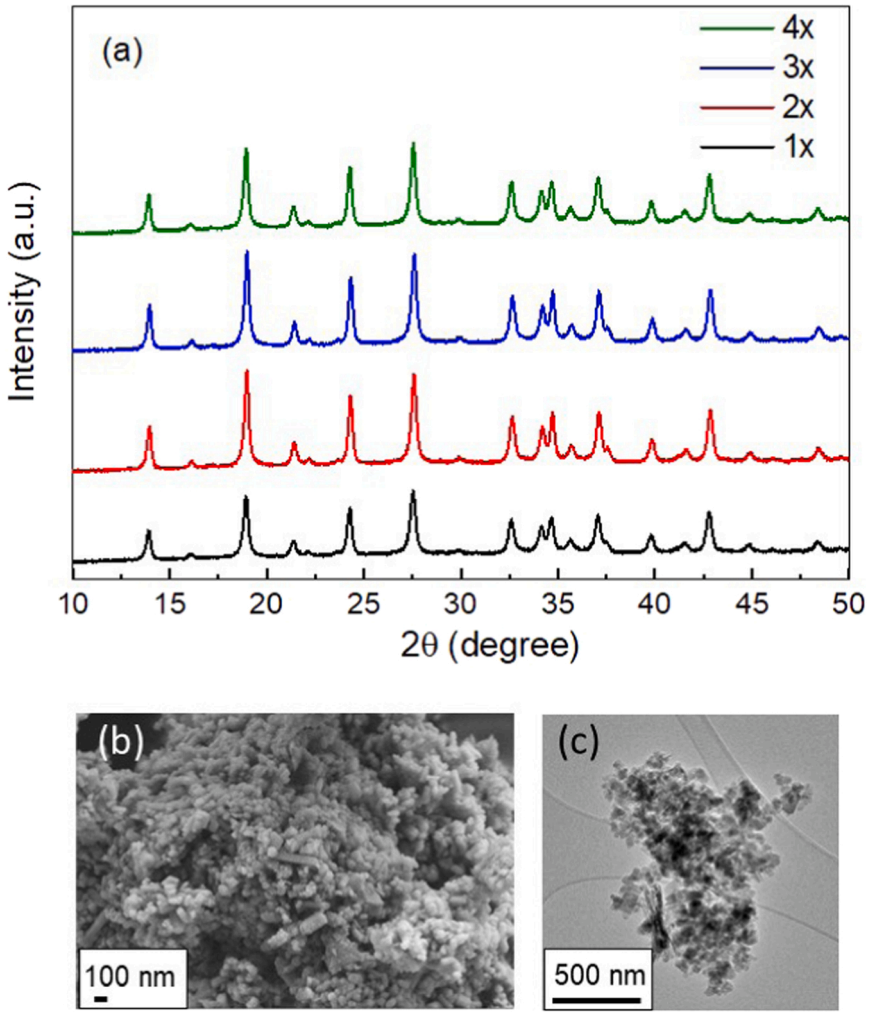

Fig. 2. (a) XRD patterns of cancrinite samples prepared in the different scale up experiments, (b) typical SEM image and (c) typical TEM image of the samples in (a).

Table 1
Si/Al ratios, SO_3 content, BET (S_{BET}) and external (S_{EXT}) surface areas and XRD crystalline sizes of cancrinite prepared at different scaling factors.

Scaling factor	Si/Al ratio	SO_3 (wt %)	S_{BET} (m^2 g^{-1})	S_{EXT} (m^2 g^{-1})	XRD crystallite size (nm)
1x	1.02	5.59	63	54	31
2x	1.02	5.65	57	51	36
4x	1.02	5.70	62	55	38
8x	1.02	5.66	63	55	38

the samples prepared at different scaling factors are shown in Fig. 3. The isotherms were type IIb isotherms according to the refined IUPAC classification of adsorption isotherms [30]. Such isotherms are observed for aggregated powders, and they are characterized by H3 hysteresis with no plateau at high relative pressures. The results further confirm that the zeolite micropores are inaccessible to the nitrogen molecules and that the samples contained textural mesoporosity with a mesopore peak centered at ca. 25 nm. The isotherms and the pore-size distributions, together with the results in Table 1, indicate that the samples prepared in the scale up experiments have remarkably similar compositional and textural characteristics.

The highly reproducible, cost-efficient, and scalable method reported for the synthesis of nanosized cancrinite with high external surface area makes this material an interesting candidate for adsorption applications. In particular, zeolites have shown potential as materials for CO_2 capture [31]. CO_2 capture under ambient temperatures at low CO_2 partial pressures is an important but challenging process. Zeolite F has been reported to achieve 80–85% CO_2 saturation at very low absolute pressure with good selectivity over N_2 and CH_4 [32]. We have measured the CO_2 adsorption at 25 °C using in situ FTIR spectroscopy (Fig. 4 and Fig. S4, Supporting Information). The method allows to differentiate between physisorbed and chemisorbed CO_2 [33]. The CO_2 physisorption on cancrinite (4x sample) at CO_2 pressures between 1.2 and 100 torr is shown in Fig. 4. The amount of CO_2 adsorbed increases dramatically with increasing equilibrium pressure indicating that the as made cancrinite zeolite could potentially be used as a low-cost adsorbent for CO_2 capture at very low CO_2 concentrations. Further, CO_2 and N_2 adsorption isotherms at 25 °C were measured conventionally (Fig. 5). Based on the single gas adsorption isotherms, the nanosized cancrinite zeolite exhibits significantly higher equilibrium CO_2 uptake (0.32 mmol g^{-1}) compared to the corresponding equilibrium N_2 uptake (0.02 mmol g^{-1}) at 100 kPa, suggesting that the interaction between cancrinite and CO_2 is stronger than that between cancrinite and N_2 [32]. The CO_2 adsorption capacity of as made nanosized cancrinite was also ca. three times higher than the value reported for the fly ash derived micron-sized cancrinite, 0.13 mmol g^{-1} [16]. The latter could be further improved by amine functionalization.

4. Conclusions

This work demonstrates that single phase cancrinite zeolite can be

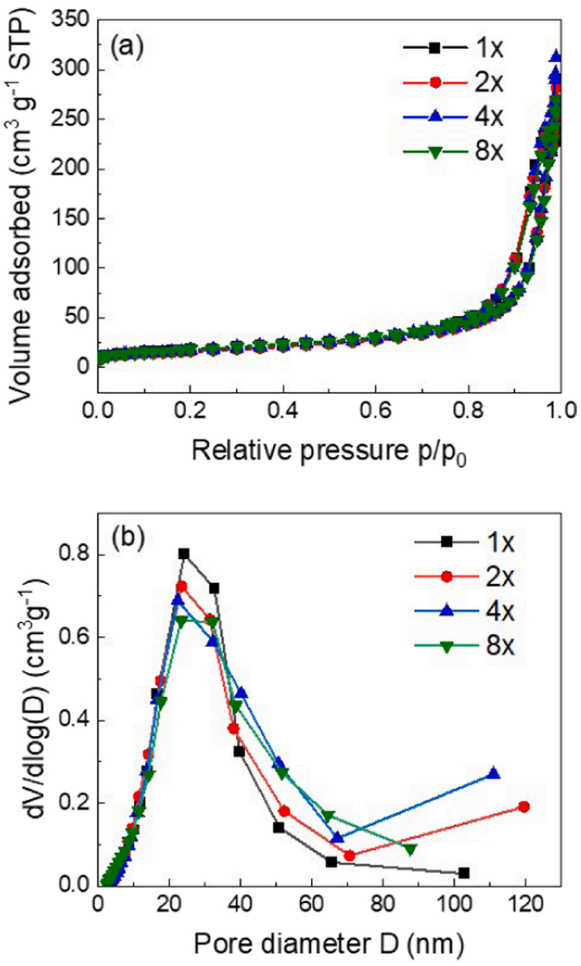

Fig. 3. (a) Nitrogen adsorption desorption isotherms of cancrinite zeolites prepared in the scale up experiments and (b) corresponding BJH pore-size distributions.

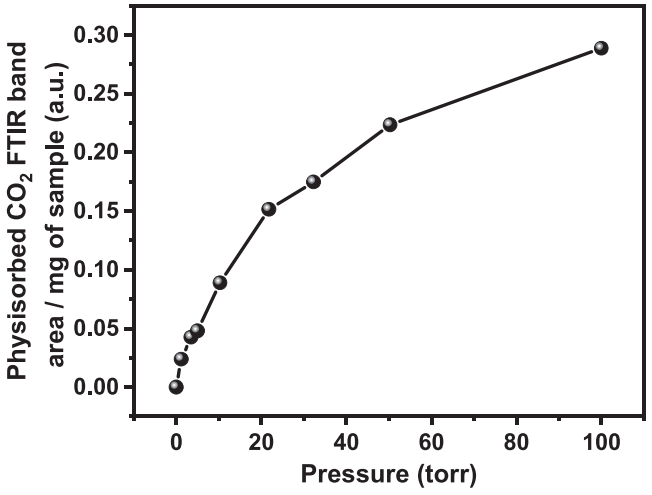

Fig. 4. Physisorbed CO_2 at different pressures (1.2–100 torr) on cancrinite calculated based on the area of the FTIR band at 2350 cm^{-1} (the intensity of the IR bands was normalized to the mass of the sample).

prepared by a cost-efficient solvent-free method using geophagic clay as raw material. The cancrinite morphology could be controlled by the trace water-bearing solid in the raw solid mixture used, sodium carbonate decahydrate or aluminum sulfate octadecahydrate. The latter is

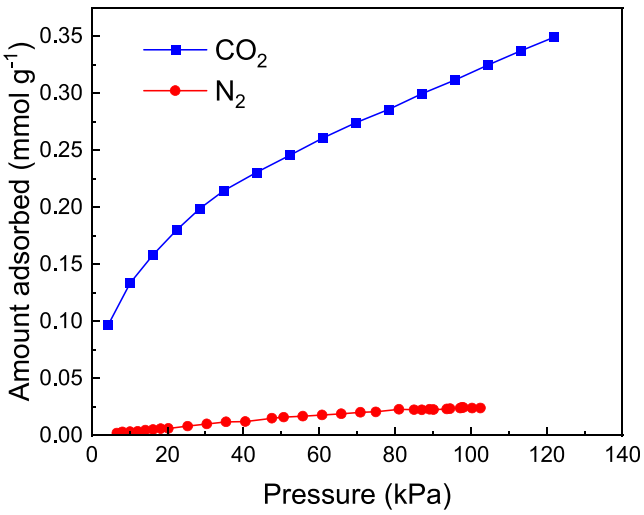

Fig. 5. CO_2 and N_2 adsorption isotherms of cancrinite measured at 25 °C.

used for the first time in a zeolite solvent-free synthesis method with the benefits of fast nucleation and suppressed crystal growth. The optimized synthesis based on the use of clay, sodium hydroxide and aluminum sulfate octadecahydrate (6 h treatment at 150 °C) provided cancrinite with remarkably consistent chemical and textural characteristics for scale up synthesis using scale factors of 1x, 2x, 4x and 8x. The benefits of the synthesis reported include the use of cheap raw materials, high yields, reduced alkaline waste, short synthesis times, and scalability. Although autoclaves were used in this work, safer reactor vessels could be used instead due to the solvent-free nature of the synthesis. The cancrinite zeolite prepared showed potential as a low-cost adsorbent for CO_2 capture at very low CO_2 concentrations.

CRediT authorship contribution statement

Ifeoma V. Joseph: Conceptualization, Methodology, Visualization, Investigation, Validation, Funding acquisition, Writing – review & editing. **Aidan M. Doyle**: Project administration, Supervision, Writing – review & editing. **Abdallah Amedlous:** Investigation, Visualization, Writing – review & editing. **Svetlana Mintova**: Supervision, Writing – review & editing. **Lubomira Tosheva:** Supervision, Visualization, Conceptualization, Writing – original draft, Writing – review & editing.

Declaration of Competing Interest

The authors declare that they have no known competing financial interests or personal relationships that could have appeared to influence the work reported in this paper.

Acknowledgements

This research was supported by the Schlumberger Foundation Stitching Fund. We acknowledge the support of the Henry Royce Institute for advanced materials with the TEM analysis, EPSRC Grant Number EP/R00661X/1.

Appendix A. Supporting information

Supplementary data associated with this article can be found in the online version at doi:10.1016/j.mtcomm.2022.103879.

References

[1] R.M. Barrer, Hydrothermal Chemistry of Zeolites, Academic Press, London, 1982.

[2] X.J. Meng, F.S. Xiao, Green routes for synthesis of zeolites, Chem. Rev. 114 (2) (2014) 1521–1543.
[3] Q.M. Wu, X.J. Meng, X.H. Gao, F.S. Xiao, Solvent-free synthesis of zeolites: mechanism and utility, Acc. Chem. Res. 51 (6) (2018) 1396–1403.
[4] L.M. Ren, Q.M. Wu, C.G. Yang, L.F. Zhu, C.J. Li, P.L. Zhang, H.Y. Zhang, X.J. Meng, F.S. Xiao, Solvent-free synthesis of zeolites from solid raw materials, J. Am. Chem. Soc. 134 (37) (2012) 15173–15176.
[5] Q.M. Wu, X.L. Liu, L.F. Zhu, L.H. Ding, P. Gao, X. Wang, S.X. Pan, C.Q. Bian, X. J. Meng, J. Xu, F. Deng, S. Maurer, U. Muller, F.S. Xiao, Solvent-free synthesis of zeolites from anhydrous starting raw solids, J. Am. Chem. Soc. 137 (3) (2015) 1052–1055.
[6] W. Luo, X.Y. Yang, Z.R. Wang, W.F. Huang, J.Y. Chen, W. Jiang, L.J. Wang, X. W. Cheng, Y.H. Deng, D.Y. Zhao, Synthesis of ZSM-5 aggregates made of zeolite nanocrystals through a simple solvent-free method, Microporous Mesoporous Mater. 243 (2017) 112–118.
[7] H. Li, X. Liu, S.Q. Qi, L.L. Xu, G.S. Shi, Y.H. Ding, X.Y. Yan, Y. Huang, J.X. Geng, Graphene oxide facilitates solvent-free synthesis of well-dispersed, faceted zeolite crystals, Angew. Chem. Int. Ed. 56 (45) (2017) 14090–14095.
[8] Z.Y. Liu, D. Wu, S. Ren, X.Q. Chen, M.H. Qiu, X. Wu, C.G. Yang, G.F. Zeng, Y. H. Sun, Solvent-free synthesis of c-Axis oriented ZSM-5 crystals with enhanced methanol to gasoline catalytic activity, Chemcatchem 8 (21) (2016) 3317–3322.
[9] W.Z. Gao, C.C. Amoo, G.H. Zhang, M. Javed, B. Mazonde, C.X. Lu, R.Q. Yang, C. Xing, N. Tsubaki, Insight into solvent-free synthesis of MOR zeolite and its laboratory scale production, Microporous Mesoporous Mater. 280 (2019) 187–194.
[10] V. Wernert, O. Schaef, L. Aloui, C. Chassigneux, F. Ayari, D.B. Chehimi, R. Denoyel, Cancrinite synthesis from natural kaolinite by high pressure hydrothermal method: application to the removal of Cd2+ and Pb2+ from water, Microporous Mesoporous Mater. 301 (2020).
[11] A.Q. Selim, E.A. Mohamed, M.K. Seliem, A.M. Zayed, Synthesis of sole cancrinite phase from raw muscovite: characterization and optimization, J. Alloy. Compd. 762 (2018) 653–667.
[12] S.M. Seo, D. Kim, J.H. Kim, Y.J. Lee, K.M. Roh, I.M. Kang, A simple synthesis of nitrate cancrinite from natural bentonite, J. Porous Mater. 25 (6) (2018) 1561–1565.
[13] M. Esaifan, L.N. Warr, G. Grathoff, T. Meyer, M.T. Schafmeister, A. Kruth, H. Testrich, Synthesis of hydroxy-sodalite/cancrinite zeolites from calcite-bearing kaolin for the removal of heavy metal ions in aqueous media, Minerals 9 (8) (2019).
[14] R.J. Zheng, X.Z. Feng, W.S. Zou, R.H. Wang, D.Z. Yang, W.F. Wei, S.Y. Li, H. Chen, Converting loess into zeolite for heavy metal polluted soil remediation based on “soil for soil-remediation” strategy, J. Hazard. Mater. 412 (2021).
[15] T.H. Dang, X.H. Nguyen, C.L. Chou, B.H. Chen, Preparation of cancrinite-type zeolite from diatomaceous earth as transesterification catalysts for biodiesel production, Renew. Energy 174 (2021) 347–358.
[16] A. Dindi, D.V. Quang, M.R.M. Abu-Zahra, CO_2 adsorption testing on fly ash derived cancrinite-type zeolite and its amine-functionalized derivatives, Environ. Prog. Sustain. Energy 38 (1) (2019) 77–88.
[17] W. Qiu, Y. Zheng, Removal of lead, copper, nickel, cobalt, and zinc from water by a cancrinite-type zeolite synthesized from fly ash, Chem. Eng. J. 145 (3) (2009) 483–488.
[18] Database of Zeolite Structures. ⟨http://www.iza-structure.org/databases/⟩ (Accessed 25 November 2021).
[19] N.V. Chukanov, S.M. Aksenov, R.K. Rastsvetaeva, Structural chemistry, IR spectroscopy, properties, and genesis of natural and synthetic microporous cancrinite- and sodalite-related materials: a review, Microporous Mesoporous Mater. 323 (2021).
[20] J.C. Buhl, V. Petrov, The hydrothermal synthesis of sulfate cancrinite (SO4-CAN): relations between Si-Al sources and crystal quality, Z. Fur Anorg. Und Allg. Chem. 645 (21) (2019) 1229–1239.
[21] S.L. Cheng, G.H. Zhang, M. Javed, W.Z. Gao, B. Mazonde, Y. Zhang, C.X. Lu, R. Q. Yang, C. Xing, Solvent-free synthesis of 1D cancrinite zeolite for unexpectedly improved gasoline selectivity, Chemistryselect 3 (7) (2018) 2115–2119.
[22] W.Z. Liu, T. Aldahri, S. Ren, C.C. Xu, S. Rohani, B. Liang, C. Li, Solvent-free synthesis of hydroxycancrinite zeolite microspheres during the carbonation process of blast furnace slag, J. Alloy. Compd. 847 (2020).
[23] P. Zhang, S.Q. Li, C.Q. Zhang, Solvent-free synthesis of nano-cancrinite from rice husk ash, Biomass Convers. Biorefinery 9 (3) (2019) 641–649.
[24] I.V. Joseph, L. Tosheva, G. Miller, A.M. Doyle, FAU-Type Zeolite synthesis from clays and its use for the simultaneous adsorption of five divalent metals from aqueous solutions, Materials 14 (13) (2021).
[25] L. Tosheva, A. Brockbank, B. Mihailova, J. Sutula, J. Ludwig, H. Potgieter, J. Verran, Micron- and nanosized FAU-type zeolites from fly ash for antibacterial applications, J. Mater. Chem. 22 (33) (2012) 16897–16905.
[26] C.A.R. Reyes, C. Williams, O.M.C. Alarcon, Nucleation and growth process of sodalite and cancrinite from kaolinite-rich clay under low-temperature hydrothermal conditions, Mater. Res. -Ibero-Am. J. Mater. 16 (2) (2013) 424–438.
[27] S.J. Chen, L.P. Sorge, D.K. Seo, Template-free synthesis and structural evolution of discrete hydroxycancrinite zeolite nanorods from high-concentration hydrogels, Nanoscale 9 (47) (2017) 18804–18811.
[28] L. Tosheva, V.P. Valtchev, Nanozeolites: synthesis, crystallization mechanism, and applications, Chem. Mater. 17 (10) (2005) 2494–2513.
[29] H. Awala, J.P. Gilson, R. Retoux, P. Boullay, J.M. Goupil, V. Valtchev, S. Mintova, Template-free nanosized faujasite-type zeolites, Nat. Mater. 14 (4) (2015) 447–451.
[30] Fo Rouquerol, J. Rouquerol, K.S.W. Sing, Adsorption by Powders & Porous Solids: Principles, Methodology And Applications, Academic Press, San Diego, Calif., 1999.
[31] S. Kumar, R. Srivastava, J. Koh, Utilization of zeolites as CO_2 capturing agents: Advances and future perspectives, J. Co2 Util. 41 (2020).
[32] M.R. Belani, R.S. Somani, H.C. Bajaj, Sorption of carbon dioxide, methane, and nitrogen on zeolite-F: Equilibrium adsorption study, Environ. Prog. Sustain. Energy 36 (3) (2017) 850–856.
[33] S. Komaty, A. Daouli, M. Badawi, C. Anfray, M. Zaarour, S. Valable, S. Mintova, Incorporation of trivalent cations in NaX zeolite nanocrystals for the adsorption of O-2 in the presence of CO_2, Phys. Chem. Chem. Phys. 22 (18) (2020) 9934–9942.